Dislocations in hexagonal and cubic GaN

2000 J. Phys.: Condens. Matter 12 10223

(http://iopscience.iop.org/0953-8984/12/49/322)

J. Phys.: Condens. Matter **12** (2000) 10223–10233. Printed in the UK PII: S0953-8984(00)17492-2

Dislocations in hexagonal and cubic GaN

A T Blumenau†‡, J Elsner†‡, R Jones†, M I Heggie§, S Öberg‖,
T Frauenheim‡ and P R Briddon¶

† School of Physics, The University of Exeter, Exeter EX4 4QL, UK
‡ Theoretische Physik, Universität Paderborn, 33095 Paderborn, Germany
§ CPES, The University of Sussex, Falmer, Brighton BN1 9QJ, UK
‖ Department of Mathematics, Luleå University of Technology, Luleå S-97187, Sweden
¶ Department of Physics, The University of Newcastle upon Tyne, Newcastle upon Tyne NE1 7RU, UK

Received 28 September 2000

Abstract. The structure and electronic activity of several types of dislocations in both hexagonal and cubic GaN are calculated using first-principles methods. Most of the stoichiometric dislocations investigated in hexagonal GaN do not induce deep acceptor states and thus cannot be responsible for the yellow luminescence. However, it is shown that electrically active point defects, in particular gallium vacancies and oxygen-related defect complexes, can be trapped at the stress field of the dislocations and may be responsible for this luminescence. For cubic GaN, we find the ideal stoichiometric 60° dislocation to be electrically active and the glide set to be more stable than the shuffle. The dissociation of the latter is considered.

1. Introduction

The blue-light emission arising from a large band gap (3.4 eV) in hexagonal GaN plays an important role in today's optoelectronics [1]. Cubic GaN is especially promising for laser devices, since it is much easier to cleave, and while the development of devices is still at an early stage, the first light-emitting diodes have already been constructed [2, 3].

Deep electronic states in the band gap induced by extended defects, such as dislocations, can significantly alter the optical performance. This becomes extremely important in laser devices where parasitic components in the emission spectrum are highly undesirable. Moreover, point defects can be trapped in the dislocation stress field and the resulting electrostatic field can then lead to electron scattering and affect the electron mobility. A model for this mechanism in hexagonal GaN has been given by Look and Sizelove [4]. Therefore, a detailed understanding of the microstructure of dislocations, their interaction with point defects and the implications for electronic and optical properties is highly desirable.

In section 2, we describe details of the methods used while section 3 contains a short overview of previous work on dislocations in hexagonal GaN. Recent results on cubic GaN are contained in section 4.

2. Computational methods

We used the two computational methods, *scc-DFTB* (**s**elf-**c**onsistent **c**harge **d**ensity-**f**unctional-based **t**ight-**b**inding method) and *AIMPRO* (*ab initio* **m**odelling **pro**gram) to investigate the properties of dislocations in GaN.

0953-8984/00/4910223+11$30.00

The *scc-DFTB* method is a tight-binding method using a minimal basis of atomic orbitals (linear combination of atomic orbitals, LCAO). The two-centre Hamiltonian and overlap matrix elements are obtained from atom-centred valence electron orbitals and the atomic potentials from single-atom density functional calculations. Exchange and correlation contributions in the total energy as well as the core–core repulsion are taken into account by a repulsive pair potential. The latter is obtained by comparison with density functional calculations. Thus this scheme can be seen as an approximate density functional scheme. Unlike other tight-binding methods, *scc-DFTB* allows charge redistributions which are taken into account using a second-order self-consistent charge extension. Details are given in previous work [5].

The *AIMPRO* method uses the pseudopotentials of Bachelet, Hamann and Schlüter [6] and a Gaussian basis set and has been described in detail elsewhere [7]. This method requires greater computing resources and thus in this work, geometrical optimization is often carried out using *scc-DFTB*.

3. Dislocations in hexagonal GaN

3.1. Threading edge dislocations

In hexagonal GaN grown by MOCVD on (0001) sapphire, edge dislocations (10^8–10^{11} cm^{-2}) are the dominant species and are thought to arise during growth from the collisions of islands [8]. The pure edge dislocations lie on $\{10\bar{1}0\}$ planes and possess Burgers vectors $\boldsymbol{b} = \boldsymbol{a} = [1\bar{2}10]/3$.

Figure 1 shows the relaxed core of the threading edge dislocation and table 1 the corresponding bond lengths and angles. With respect to the perfect lattice the distance between columns (1/2) and (3/4) is 9% contracted while the distance between columns (9/10) and (7/8) is stretched by 13%. The structure has been confirmed by Xin *et al* [9] using high-resolution Z-contrast imaging. Consistent with our calculations, they determined a contraction/stretching of $15 \pm 10\%$ of the distances between the columns at the dislocation core. Our calculations show that, in a manner identical to the $(10\bar{1}0)$ surface, the threefold-coordinated Ga (N) atoms (Nos 1 and 2 in figure 1) relax towards sp^2 (p^3). This leads to the empty Ga dangling-bond states being pushed towards the conduction band minimum, CBM, and filled lone pairs on N atoms displaced to the valence band maximum, VBM. Thus using *scc-DFTB* we find full-core threading edge dislocations to be free from deep gap states, and thus they are not charged. In contrast, plane-wave scf calculations by Wright and Gossner [10] found that the full-core edge

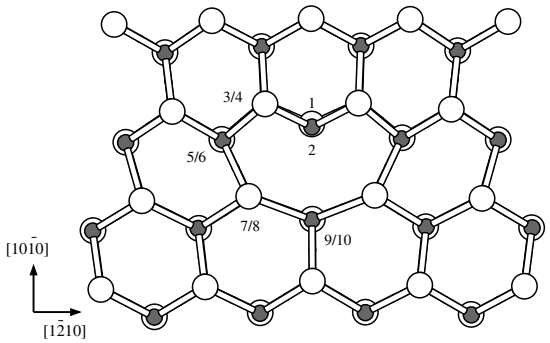

Figure 1. A top view (along [0001]) of the relaxed core of the threading edge dislocation in hexagonal GaN ($\boldsymbol{b} = (1/3)[1\bar{2}10]$). The threefold-coordinated atoms 1 (Ga) and 2 (N) adopt a hybridization similar to that of the $(10\bar{1}0)$ surface atoms. The distance between columns (1/2) and (3/4) is contracted by 9% while the distance between (7/8) and (9/10) is stretched by 13%.

Table 1. Bond lengths and bond angles for the most distorted atoms at the core of the threading edge dislocation ($\boldsymbol{b} = (1/3)[1\bar{2}10]$) in hexagonal GaN. Numbers in brackets give the average bond lengths. Atom numbers refer to figure 1.

Atom	Atom type	Coordination	Bond lengths in Å	Bond angles
1	Ga	3	1.85–1.86 (1.85)	112°–118°
2	N	3	1.88–1.89 (1.86)	106°–107°
3/4	Ga/N	4	1.86–1.95 (1.91)	97°–119°
5/6	Ga/N	4	1.92–2.04 (1.97)	100°–129°
7/8	Ga/N	4	1.94–2.21 (2.06)	94°–125°
9/10	Ga/N	4	1.95–2.21 (2.11)	100°–122°

dislocation possesses states 0.75 eV below the CBM. However, recent Monte Carlo simulations for different background dopant densities based on similar calculations [11] have shown that no significant charge accumulation occurs at the dislocation even in heavily n-doped material.

Our calculations show that the line energy of the edge dislocation is 2.19 eV Å^{-1} and is considerably lower than that found for the open screw dislocation. This can be explained by the smaller number of threefold-coordinated atoms in the core of the edge dislocation compared to the open-core screw dislocation, and to a smaller elastic component.

We also investigated whether the energy of the threading edge dislocation could be lowered by removing the most distorted core atoms. However, removal of either of the labelled columns in figure 1 leads to a considerably higher line energy. This implies that the threading edge dislocation should exist with a full core. Recent Z-contrast imaging and EELS experiments by Xin *et al* [12] show that the vast majority of edge dislocations have indeed a full core. For n-type GaN they find the concentration of Ga vacancies in the core to be less than 15%.

We then investigated the interaction of deep acceptors with the dislocation core. In GaN, vacancy–oxygen defect complexes, namely V_{Ga}–$(O_N)_2$ and V_{Ga}–(O_N), act as single and double acceptors, respectively. If these defects were trapped in the stress field of a dislocation, then we would expect the dislocation to appear electrically active [13]. Simple considerations suggest that V_{Ga}–$(O_N)_n$ would be bound to the dislocation core. This is because an O atom inserted into the N site at the core can form a bridge bond with two Ga neighbours, while the removal of a neighbouring Ga atom leaves two N dangling bonds as opposed to four in the bulk. Our calculations find the resulting formation energies of these defects at the dislocation core and in the dislocation stress field to be significantly lower than in bulk material (see earlier work for more details [13]). Thus, if oxygen is mobile, the core of the dislocation will spontaneously oxidize. Thus, we anticipate that electrically active donor and acceptor pairs will be trapped at the core and in the dislocation stress field, possibly giving rise to a negatively charged dislocation line in n-type material in agreement with temperature-dependent Hall measurements [4]. V_{Ga} and V_{Ga}–$(O_N)_n$ are good candidates for explaining the yellow luminescence in GaN.

3.2. Threading screw dislocations

The most common screw dislocations in hexagonal material have Burgers vectors $\boldsymbol{b} = \boldsymbol{c} =$ [0001] and thread the epilayer. They probably arise from the collision of islands during growth [8].

We consider first a screw dislocation with a full core [14]. Both the *AIMPRO* and the *scc-DFTB* method found heavily distorted bond lengths (as much as 0.4 Å) yielding deep gap states ranging from 0.9 to 1.6 eV above the VBM, and shallow gap states at 0.2 eV below the

CBM. Further analysis of the states revealed that the lower states near the VBM are localized on N core atoms, whereas the states below the CBM are localized on core atoms but have mixed Ga and N character. Therefore the full-core screw dislocation is electrically active and could act as a non-radiative centre [14]. This dislocation has subsequently been observed experimentally by Xin *et al* [9] using high-resolution Z-contrast imaging. Further studies using scanning electron microscopy, atomic force microscopy and transmission electron microscopy in combination with photoluminescence have recently confirmed that these dislocations act as strong non-radiative centres [15]. Earlier, Rosner *et al* came to similar conclusions [16].

The line energy of the closed screw was found from a supercell calculation to be 4.88 eV Å^{-1}. This large energy reflects the heavy bond distortion within the core.

Similar calculations were carried out with the hexagonal core removed. This gives a core with a narrow opening of approximately 7.2 Å. The atoms on the walls adopt threefold coordinations similar to those found on the $(10\bar{1}0)$ surface. Thus Ga (N) atoms develop sp^2 (p^3) hybridizations which lower the surface energy and clear the gap of deep states. We find now only shallow gap states which are induced by the distortion arising from the Burgers vector. This was verified by comparison with the undistorted $(10\bar{1}0)$ surface which shows no shallow states.

Bond distortion in the open-core screw dislocation (maximum of 0.2 Å) is significantly less than in the full-core screw dislocation. It is therefore not surprising that the calculated line energy of 4.55 eV Å^{-1} is lower than that of the full-core screw dislocation. The energy required to form the surface at the wall is compensated by the energy gained by reducing the strain. However, a further opening gave a higher line energy and we conclude that the equilibrium diameter is approximately 7.2 Å. An opening of the screw has been observed by Liliental-Weber [17] who found some of the screw dislocations to have holes which are three atomic rows wide.

4. 60° dislocations in cubic GaN

There are only very few experimental results on dislocations in cubic GaN. However, there are reports of 60° dislocations, twins and stacking faults seen by TEM in cubic GaN grown on GaAs(001) [19]. The 60° dislocations emerge from the GaN/GaAs interface. So far, nothing is known concerning their structures.

As *et al* [20] find from Hall measurements on Si-doped cubic GaN that the electron mobility increases with increasing Si doping for electron concentrations smaller than 3×10^{19} cm^{-3}. For higher concentrations the mobility decreases again. This behaviour is characteristic for electron trapping at dislocations suggesting that dislocations are active [4]. Temperature-dependent Hall measurements on undoped material showed it to be p-type ($p \sim 10^{16}$ cm^{-3}) with an acceptor level at ∼166 meV above the VBM [20]. This indicates that many acceptors are neutral at room temperature and leads to an acceptor concentration of $\sim 10^{18}$ cm^{-3}, which is comparable with the density of dislocation core atoms. One problem is that the electrical properties might be related to interfaces between cubic and hexagonal phases.

4.1. Undissociated 60° *dislocations*

60° dislocations are of mixed edge and screw character with a Burgers vector inclined at an angle of 60° to the direction of the dislocation line. In cubic GaN, accordingly, we have a line direction of $[01\bar{1}]$ and a Burgers vector of $\boldsymbol{b} = [1\bar{1}0]/2$. There are two types of 60° dislocations in cubic GaN, namely: shuffle and glide. Both types contain cores of gallium or nitrogen atoms and thus there are four different dislocations [21].

We first investigate the shuffle type. Figure 2 (left) shows the projection of the relaxed 60° shuffle dislocation with a N core. The dislocation lies along $[01\bar{1}]$ and is normal to the projection plane. The bond lengths and bond angles of the threefold-coordinated N core atom 1 are given in table 2. With respect to the perfect lattice the bonds between the core atom 1 and its next Ga neighbours (2/3) are 7% compressed while those between 4, 5, 6, 7 and 8 are expanded 7%. Although the threefold-coordinated N core atoms 1 relax along $-[111]$, they remain sp^3 like. We therefore expect the dangling bonds of those atoms to induce deep gap states. Indeed, as shown in figure 3, our calculations reveal dislocation-related states giving rise to a band (a) above the VBM as well as states (b) just above the Ga 3d band. For an uncharged dislocation line, band (a) is approximately half-filled and lies ∼0.2 eV above the VBM. Its width is about ∼0.2 eV. Thus in p-type GaN, we expect the dislocation band to act as an acceptor. The position and character of this band appears to agree with the results of As *et al* [20] although further studies are called for.

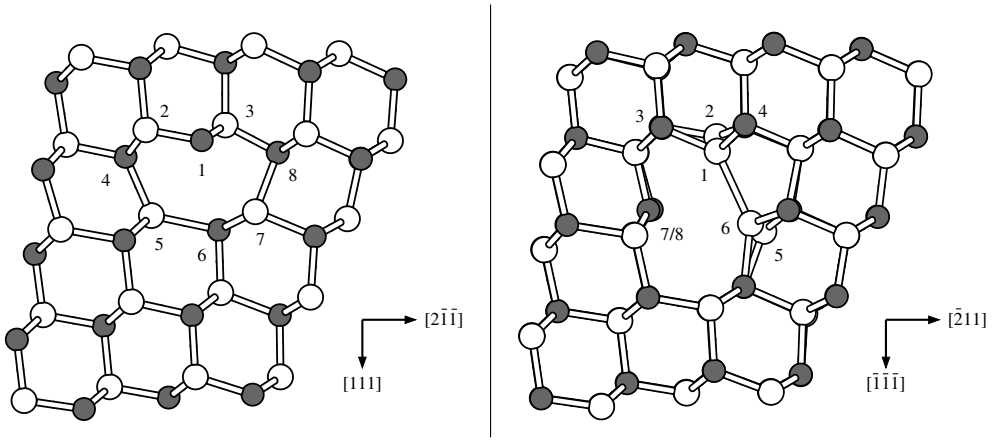

Figure 2. The top view (along $[01\bar{1}]$) of the relaxed core of the two different types of 60° shuffle dislocation in cubic GaN. Left: the N core dislocation. The core atom 1 (N) is threefold coordinated and sp^3 hybridized. Thus its dangling bond lies in the [111] direction. All other atoms shown are fourfold coordinated. Right: the Ga core dislocation. This structure is double periodic with a bond between the two Ga atoms 1 and 6 but no bond between 2 and 5.

Table 2. Bond lengths and bond angles for the nitrogen core atom of the 60° shuffle dislocation in cubic GaN. Numbers in brackets give the averages. The atom number refers to figure 2 (left).

Atom	Atom type	Coordination	Bond lengths in Å	Bond angles
1	N	3	1.81–1.84 (1.82)	105°–122° (114°)

The relaxed Ga core 60° shuffle dislocation is shown in figure 2 (right). The dislocation lies along $[01\bar{1}]$ and thus is normal to the projection plane. The corresponding bond angles of all threefold-coordinated atoms are given in table 3. Unlike for the N core type, the Ga–N bonds between columns (5/6) and (7/8) (corresponding to 5 and 6 for the dislocation of N core type) are broken, allowing those columns to relax further outwards. Every second threefold-coordinated Ga atom along the dislocation line is distorted inwards. This leads to a double periodic structure with a bond between the two Ga atoms 1 and 6, but no bond between 2 and 5. Due to this we also find a corresponding charge modulation of ±0.2 electrons along the dislocation line. The distances between the threefold-coordinated atoms are shown in table 4.

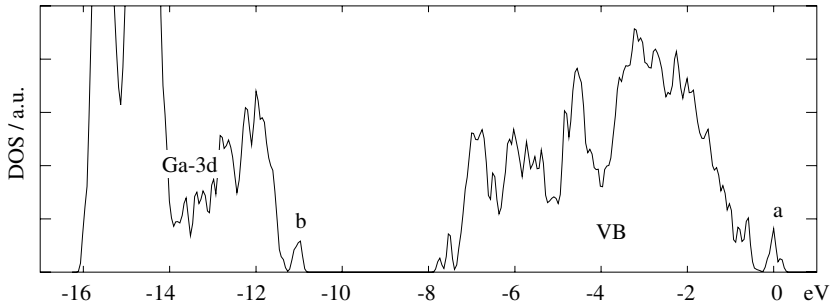

Figure 3. The calculated density of states (DOS) of the 60° shuffle dislocations with the N core (cubic GaN). The dislocation induces states (b) in the gap between the low-lying states of the Ga 3d electrons and the valence band as well as states (a) above the VBM. If we scale the band gap (the CBM is not shown here) to fit the experimental value, we find (a) to be 0.2 eV above the VBM. 0 eV refers to the Fermi level for an uncharged dislocation line. Thus the dislocation-induced band (a) is then half-filled.

Table 3. Bond angles for all threefold-coordinated atoms at the core of the 60° shuffle dislocation with a Ga core (cubic GaN). Numbers in brackets give the averages. Atom numbers refer to figure 2 (right).

Atom	Atom type	Coordination	Bond angles
1	Ga	3	99°–110° (105°)
2	Ga	3	110°–121° (116°)
5	Ga	3	112°–124° (117°)
6	Ga	3	100°–110° (104°)
7	N	3	108°–121° (115°)
8	N	3	105°–117° (112°)

Table 4. Distances between the threefold-coordinated atoms at the core of the 60° shuffle dislocation with a Ga core (cubic GaN). Atom numbers refer to figure 2 (right).

Distance between atoms		Distance in Å
1 (Ga)–6 (Ga)	(Reconstructed bond)	2.53
2 (Ga)–5 (Ga)	(No bond)	3.33
6 (Ga)–8 (N)	(Broken bond)	3.33
5 (Ga)–7 (N)	(Broken bond)	3.66

Examination of the density of states in figure 4 reveals a dislocation band (a) near the VBM and further states (b) around the mid-gap position. For an uncharged dislocation line, band (a) is partially filled and lies ∼0.3 eV above the VBM with a width of ∼0.2 eV. Thus, as in the case of the N core dislocation, in p-type GaN we can expect the dislocation band to act as an acceptor.

Removing the column of threefold-coordinated N atoms (1) from the 60° shuffle dislocation with N core (figure 2 (left)) leads to a glide dislocation with a Ga core. Figure 5 shows its corresponding relaxed structure. We find reconstructed Ga–Ga bonds with a length of 2.37 Å between atoms 1 and 2. Table 5 gives the bond lengths and angles of the Ga–N bonds of the two Ga atoms 1 and 2. For the neutral charge state, the reconstructed core structure gives rise to a filled band 0.3 eV above the VBM and a half-filled band 1.6 eV above the VBM and thus the dislocation will be positively charged in p-type material. We find the formation energy of the 60° glide dislocation (Ga core) to be by at least 0.34 eV $Å^{-1}$ lower than that of

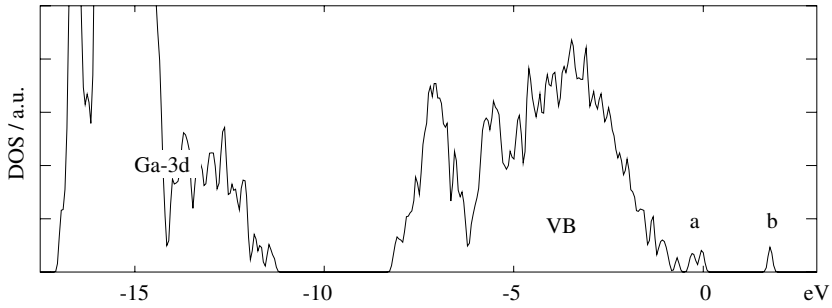

Figure 4. The calculated density of states (DOS) of the 60° shuffle dislocations with a Ga core (cubic GaN). For an uncharged dislocation line (Fermi level at 0 eV) we find a partially filled band (a) 0.3 eV above the VBM and further empty states (b) at the mid-gap position (both scaled as described in figure 3).

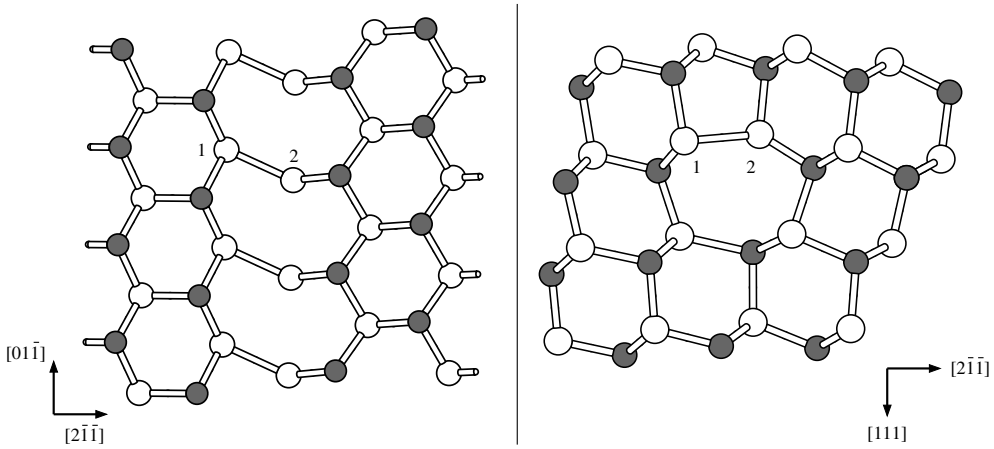

Figure 5. The relaxed core of the 60° glide dislocation with a Ga core (cubic GaN.). Left: a view projected onto the {111} glide plane. The dislocation lies vertically along [01$\bar{1}$]. We find a bond reconstruction between the core atoms (types 1 and 2). Atom 1 (Ga) is fourfold coordinated with three N atoms and one Ga atom (2). Atom 2 (Ga) is only threefold coordinated with two neighbouring N atoms and one Ga atom (1). Right: the top view along [01$\bar{1}$].

Table 5. Bond lengths and bond angles of the two gallium core atoms of the 60° glide dislocation with their nitrogen neighbours (cubic GaN). Numbers in brackets give the averages. Atom numbers refer to figure 5. For atom 2 only one angle is given since it has only two neighbouring N atoms.

Atom	Atom type	Coordination	Bond lengths in Å	Bond angles
1	Ga	4	1.89–2.03 (1.97)	109°–115° (111°)
2	Ga	3	1.84–1.92 (1.88)	117°

the 60° shuffle dislocation (N core) even for N-rich growth conditions. Thus the Ga core glide type is more stable than the corresponding N core shuffle type.

So far, no calculations concerning the 60° glide dislocation with an N core have been performed, but we can expect it to be electrically active as well and probably more stable than the corresponding shuffle type.

4.2. The interaction of impurities with the 60° *shuffle dislocation*

We found that the nitrogen vacancy (V_N) and O_N are bound (position 1 in figure 2) to the N core 60° shuffle dislocation with energies of 4.4 and 2.2 eV respectively. These contrast with C_N which was found to be unbound. We thus conclude that oxygen and nitrogen vacancies are likely to accumulate at the dislocation core.

To investigate further the effects of O_N on the electronic structure, we increased the O concentration from 1/4 to 3/4 of all core atoms at position 1 in figure 2. This filled up the dislocation band but did not lead to any significant change in its position.

4.3. The dissociation of the 60° *Ga core dislocation*

In many cubic materials, the 60° glide dislocation dissociates into two partial dislocations lying on the {111} glide plane and separated by an intrinsic stacking fault [21]. The dissociation reaction is given by

$$\frac{1}{2}[1\bar{1}0] \longrightarrow \frac{1}{6}[1\bar{2}1] + \frac{1}{6}[2\bar{1}\bar{1}] \tag{1}$$

where the term on the right-hand side corresponds to a 30° partial and the second a 90° partial dislocation. We modelled the two partials with *scc-DFTB* in a 520-atom supercell–cluster hybrid, periodic along the dislocation line, but hydrogen terminated in the remaining directions. We were able to compare dislocations with different separations between the two partial dislocations. Figure 6 shows the relaxed Ga core structures projected onto the glide plane for three different separations. The structures for the isolated partials without any interaction were obtained from additional models containing only one partial dislocation each. One can see from figure 6 that the core structures of the 30° and the 90° partials depend on their separation For the smallest separation (one spacing), the 90° partial (left) shows a single periodic bond reconstruction whereas the 30° partial (right) remains unreconstructed. For a larger separation of five spacings, we find a double periodic bond reconstruction for the 90° partial, where every second pair of Ga core atoms along the dislocation line is only weakly bound. For the same separation the core of the 30° partial shows a double periodic reconstruction as well. Here pairs of Ga atoms are bound along $[01\bar{1}]$ (bond length 2.46 Å). Finally, for very large separation we get isolated partials. The 90° partial core remains unreconstructed but the 30° partial shows a double periodic structure similar to that for a separation of five spacings. However, the reconstruction bond length is 2.81 Å, considerably larger than that for five spacings.

The change in core structures with increasing separation leads to a corresponding change in the charge at the Ga core atoms. Since our calculations were performed on a neutral cell, the charge accumulated at the partial cores is taken from the surrounding lattice. Table 6 lists the additional charge at the Ga core atoms of the two partial dislocations for different separations between the two. For the smallest separation, the charge accumulation at the undissociated 60° glide dislocation (Ga core) is given. For a separation of one spacing, only the 90° partial shows reconstructed bonds; accordingly all the bond charge is located on these. For five spacings the charge is almost equally distributed among both partials and in the limit of very large separation distances the charge at the 30° partial has 40% less charge than the 90° partial. We note that the sum of charges at the two partial cores is almost constant but slowly increases with increasing separation to reach its maximum of 0.73 electrons per 3.2 Å. Although the charge accumulation depends on the size of our model, we believe that our results show the right trend.

To learn more about the energetics of the dissociated 60° glide dislocation, we compared the formation energies of the two partials separated by a stacking fault with the formation

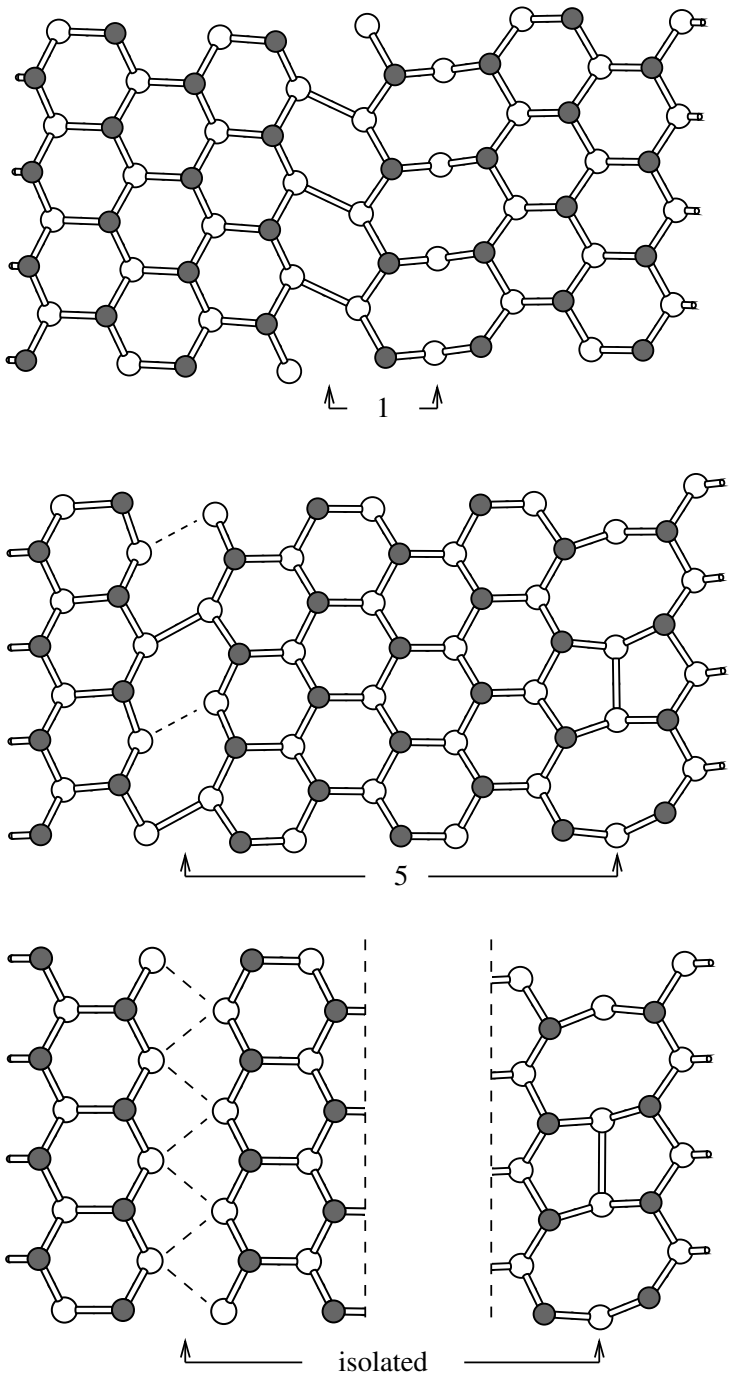

Figure 6. A view (projected onto the {111} glide plane) of the dissociated 60° glide dislocation with a Ga core. The dissociation is shown for three different distances between the partial dislocations. The arrows show the location of the partials, the 90° partial being on the left and the 30° partial on the right, separated by an intrinsic stacking fault. As discussed in the text, the bond reconstruction and geometry of the core depend on the distance between the two partials. Top: a separation of one spacing of ∼2.7 Å between the cores. Middle: a separation of five spacings of ∼2.7 Å. Bottom: isolated partials with no interaction.

Table 6. Charge accumulation at the Ga core atoms of the dissociated 60° glide dislocation depending on the separation between the partials. The separation is given in spacings of ∼2.7 Å and the charge q in elementary charge $|e|$ per 3.2 Å. For a separation of 0 Å we have the undissociated 60° glide dislocation and thus cannot distinguish between charge at the 30° and 90° partial cores. ∞ represents two isolated partials with no interaction.

Separation (2.7 Å):	0	1	5	∞
q (30° partial):	—	0.0	−0.37	−0.27
q (90° partial):	—	−0.68	−0.31	−0.46
$\sum q$ (30° and 90°):	−0.60	−0.68	−0.68	−0.73

energy of the undissociated 60° glide dislocation. Figure 7 shows the change in the formation energy starting from the undissociated dislocation, then dissociating into the two partials and increasing the separation distance. Isotropic elasticity theory gives two energy contributions: the reduction of the strain field and the corresponding elastic energies with increasing distance between the partials (90°–30° partial repulsion) and as a compensating effect the increase in stacking fault energy with increasing distance [21]. In addition to this, one has to consider the core energies of the undissociated dislocation and the two partials. Figure 7 shows an especially large increase in energy with separation going from zero to one spacing, and thus for the dissociation itself. This reveals the importance of the difference in core energies. So far these core energies are not determined. Also, for small distances, the electrostatic interaction between the two partials might play a role, since the core charge is then not fully screened. The detailed development of the formation energy for the first five spacings of separation cannot be explained easily, because it is heavily dependent on the core structures of the partials also—and these core structures change significantly with changing separation. Further calculations are being carried out, to investigate whether the dissociation of the 60° glide dislocation is energetically favourable.

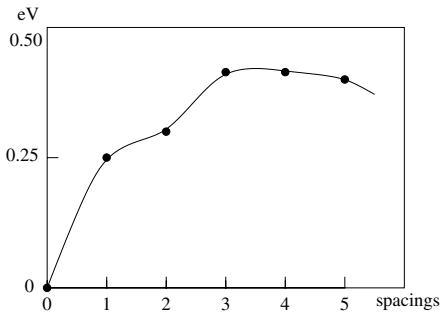

Figure 7. The total energy per Å of a system of a 90° and a 30° partial (Ga core) depending on the separation. The distances are given in spacings of ∼2.7 Å. All energies are calculated relative to the energy of the undissociated 60° dislocation. Thus we get 0 eV for a separation of 0 Å (undissociated).

5. Summary and conclusions

We have presented calculations for a variety of threading dislocations lying along $\boldsymbol{c}$ in hexagonal GaN. We found that core bonds in the full-core screw dislocation suffer a large distortion resulting in deep gap states. Open-core screw dislocations and particularly threading edge

dislocations possess a core structure similar to that of $(10\bar{1}0)$ surfaces and do not induce deep acceptor states in their impurity-free form.

Oxygen-related defect complexes, some of which are electrically active, are strongly bound to the core and in the stress field of threading edge dislocations in hexagonal GaN.

We found that 60° dislocations in cubic GaN are electrically active. The undissociated 60° dislocation with a nitrogen core can induce acceptor states roughly 0.2 eV above the VBM. Thus they are candidates for being the ∼0.166 eV acceptors observed experimentally in cubic GaN by As *et al* [20]. In the same way as dislocations in the hexagonal material, the 60° dislocations are likely to trap point defects and impurities which could alter their electrical properties. Further calculations are necessary to decide whether 60° dislocations in cubic GaN dissociate.

Acknowledgments

SÖ thanks NFR and TFR, ATB and JE thank DFG for financial support. The authors also would like to thank A F Wright, Z Liliental-Weber and Y Xin for useful and stimulating discussions.

References

[1] Nakamura S and Fasol G 1997 *The Blue Laser Diode* (Berlin: Springer)
[2] Yang H, Zheng L X, Li J B, Wang X J, Xu D P, Wang Y T and Hu X W 1999 *Appl. Phys. Lett.* **74** 2498
[3] As D J, Richter A, Busch J, Lübbers M, Mimkes J and Lischka K 2000 *Appl. Phys. Lett.* **76** 13
[4] Look D C and Sizelove J R 1999 *Phys. Rev. Lett.* **82** 1237
[5] Elstner M, Porezag D, Jungnickel G, Elsner J, Haugk M, Frauenheim T, Suhai S and Seifert G 1998 *Phys. Rev.* B **58** 7260
[6] Bachelet G B, Hamann D R and Schlüter M 1982 *Phys. Rev.* B **26** 4199
[7] Jones R and Briddon P R 1998 *Identification of Defects in Semiconductors (Semiconductors and Semimetals vol 51A)* ed M Stavola (Boston, MA: Academic) ch 6
[8] Ning X J, Chien F R and Pirouz P 1996 *J. Mater. Res.* **11** 580
[9] Xin Y, Pennycook S J, Browning N D, Nelist P D, Sivananthan S, Omnes F, Beaumont B, Faurie J-P and Gibart P 1998 *Appl. Phys. Lett.* **72** 2680
[10] Wright A F and Gossner U 1998 *Appl. Phys. Lett.* **73** 2751
[11] Leung K, Wright A F and Stechel E B 1999 *Appl. Phys. Lett.* **74** 2495
[12] Xin Y, James E M, Arslan I, Sivananthan S, Browning N D, Pennycook S J, Omnes F, Beaumont B, Faurie J-P and Gibart P 2000 *Appl. Phys. Lett.* **76** 466
[13] Elsner J, Jones R, Haugk M, Frauenheim T, Heggie M I, Öberg S and Briddon P R 1998 *Phys. Rev.* B **58** 12 571
[14] Elsner J, Jones R, Sitch P K, Porezag V D, Elstner M, Frauenheim T, Heggie M I, Öberg S and Briddon P R 1997 *Phys. Rev. Lett.* **79** 3672
[15] Hino T, Tomiya S, Miyajima T, Yanashima K, Hashimoto S and Ikeda M 2000 *Appl. Phys. Lett.* **76** 3421
[16] Rosner S J, Carr E C, Ludowise M J, Girlami G and Erikson H I 1997 *Appl. Phys. Lett.* **70** 420
[17] Liliental-Weber Z 1998 Private communication
[18] Frank F C 1951 *Acta Crystallogr.* **4** 497
[19] Kaiser S and As D J 1999 Private communication (TEM experiments)
[20] As D J, Richter A, Busch J, Schöttker B, Lübbers M, Mimkes J, Schikora D, Lischka K, Kriegseis W, Burkhardt W and Meyer B K 2000 *MRS Internet J. Nitride Semicond. Res.* **5S1** W3.81
[21] Hirth J P and Lothe J 1982 *Theory of Dislocations* 2nd edn (New York: McGraw-Hill)